Efficient Wave Energy Amplification with Wave Reflectors

Kramer, Morten Mejlhede; Frigaard, Peter Bak

Published in:
Proceedings of the Twelfth (2002) International Offshore and Polar Engineering Conference, Kitakyushu, Japan

Publication date:
2002

Document Version
Early version, also known as pre-print

Efficient Wave Energy Amplification with Wave Reflectors

Morten Kramer and Peter Frigaard
Hydraulics and Coastal Engineering Laboratory, Department of Civil Engineering, Aalborg University
Sohngaardsholmsvej 57, DK-9000 Aalborg, Denmark

ABSTRACT

Wave Energy Converters (WEC's) extract wave energy from a limited area, often a single point or line even though the wave energy is generally spread out along the wave crest. By the use of wave reflectors (reflecting walls) the wave energy is effectively focused and increased to approximately 130-140%. In the paper a procedure for calculating the efficiency and optimizing the geometry of wave reflectors are described, this by use of a 3D boundary element method. The calculations are verified by laboratory experiments and a very good agreement is found. The paper gives estimates of possible power benefit for different geometries of the wave reflectors and optimal geometrical design parameters are specified. On this basis inventors of WEC's can evaluate whether a specific WEC possibly could benefit from wave reflectors.

KEY WORDS: Wave energy converter; wave focusing.

INTRODUCTION

To extract wave energy for electricity consumption a large number of WEC's have been invented in resent years. Most of these can benefit from wave reflectors. Near the coast the waves are often depth limited due to shallow water and sufficient water depth for wave focusing is usually not available. However in the deep waters offshore, sufficient water depth and greater energy is generally available. Consequently floating WEC's of the overtopping type and devices based on the Oscillating Water Column system may possibly benefit most from floating wave reflectors.

The described problem has the point of origin in optimizing the wave reflectors for the *Wave Dragon*.

Wave Dragon

The Wave Dragon is a floating WEC of the overtopping type. It uses two patented wave reflectors to focus the waves towards a ramp. When the waves overtop the ramp the water is filled into a reservoir located above MWL. From here electricity is generated through turbines. Wave Dragon is invented by Erik Friis-Madsen from the Danish company Löwenmark F.R.I.
To choose the most efficient geometric shape of the wave reflectors the following degrees of freedom must be chosen:

- The draft and height of the reflectors
- The change in curvature along the reflectors
- The length ratio defined as L/(b - a)
- The opening ratio defined as b/a

Provisional investigations for choosing the optimal parameters have been carried out by the inventor (Kofoed *et al*, 2000; Soerensen *et al*, 2000). In the light of this the layout of the reflectors illustrated on Fig. 1 was chosen.

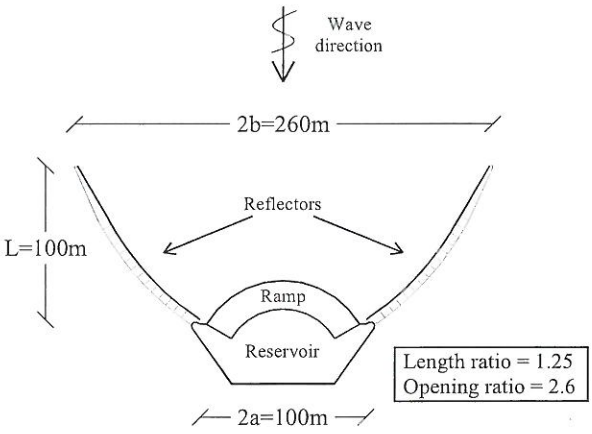

Fig. 1. Plan view of the Wave Dragon

For the setup shown on Fig. 1 the draft is about 9 meters (a little less at the tip and more by the ramp). The anchoring of Wave Dragon ensures that the propagating wave direction always is as indicated in Fig. 1 (i.e. perpendicular to the centre of the ramp).

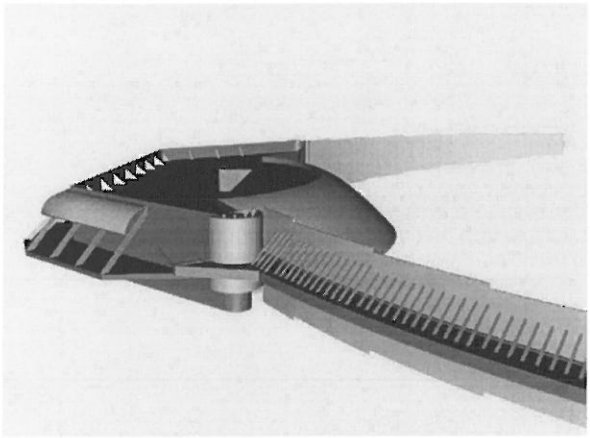

Fig. 2. Picture of Wave Dragon made by Jes Paul, Loke Film

MODEL LAYOUT

The subsequent calculations have been made to optimize the reflector layout on Fig. 1. This is done by optimizing the wave power in the cross section between two fixed reflectors, along $y \equiv 0$ and $x = \pm a$ on Fig. 3. No other parts than the reflectors are present in the wave field.

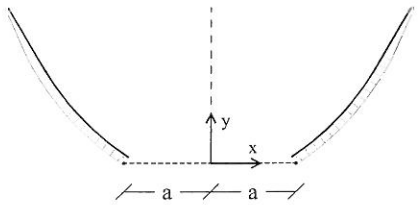

Fig. 3. Line for wave energy optimization

The efficiency of the reflectors is calculated as the actual mean power in the cross section divided by the power of the undisturbed incoming wave (i.e. the wave power that would be present if the reflectors were not present in the wave field).

$$\text{Efficiency} = \frac{\text{Actual power in cross section}}{\text{Power in incoming wave}} \ 100\% \qquad (1)$$

The importance of the length and opening ratio is investigated further. A fixed curvature, height and draft of the reflectors are chosen (as for the reflector design on Fig. 3). In order to have a more convenient set of degree of freedom the following is used as an alternative to the length and opening ratio.

1) The reflectors rotated around the point $x = \pm a$
2) The tip of the reflectors extended in the axial direction

4 positions with rotated reflectors have been tested. Relative to the original position of the reflectors the following positions have been tested: -5°, 0°, +5° and +10° (positive angle = narrower opening). This result in opening ratios from 2.3 to 2.8 and length ratios from 1.0 to 1.8.

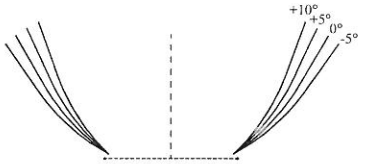

Fig. 4. Sketch of rotated reflectors

Further the length of the reflectors has been investigated. The axial length of the reflectors on Fig. 1 is 125m. This length is extended -30m, -20m, -10m, 0m and +10m.

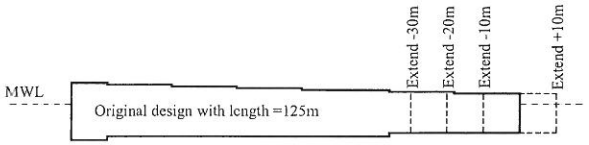

Fig. 5. Sheer plan of reflector.

WAVE SITUATIONS

The different layouts are tested in both regular waves and irregular waves. In the numerical model the layouts are tested in regular waves with periods from 4sec to 20sec (frequencies from 0.05Hz to 0.25Hz). In the laboratory two regular wave situations with periods of 5.6sec and 7.0 sec have been tested.

The layouts are tested in irregular wave situations to be found in the Danish part of the North Sea. A JONSWAP spectrum with peak enhancement factor 3.3 is used. In Table 1 the mean power in the waves are calculated per metre wave front. It is seen that in a large part of the year (47%) the waves are short and small (Hs=1m).

Table 1. Typical Danish wave situations.

Hs [m]	1	2	3	4	5
Tp [sec]	5.6	7.0	8.4	9.8	11.2
Power [kW/m]	2	12	32	66	115
Probability [%]	47	23	11	5	2

In the rest of the year, the waves are smaller than 0.5m or larger than 5.5m. The mean power in the waves is 16kW per metre wave front.

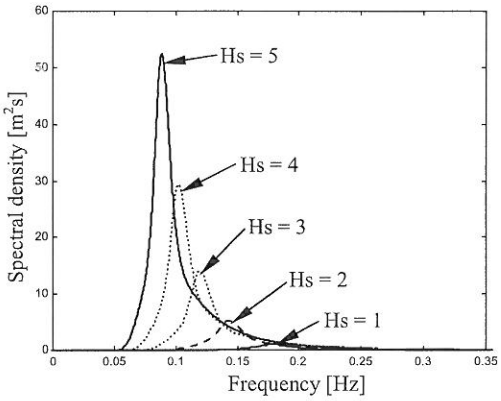

Fig. 6. Tested wave spectra

NUMERICAL MODEL

A 3D boundary element method (BEM) is applied. In BEM the meshing requirement is reduced to the structure's boundary surface, as a result it provides an efficient and accurate frequency domain solution for linear wave structure interaction problems. A source distribution technique (Wehausen & Laitone, 1960) based on potential flow theory is used to calculate the velocity potentials φ in the Laplace equation. In the following the main procedure in the calculations is given.

Solving the Laplace Equation

$$\nabla^2\varphi = 0 \qquad ,\nabla^2 = \left(\frac{\partial^2}{\partial x^2},\frac{\partial^2}{\partial y^2},\frac{\partial^2}{\partial z^2}\right) \tag{2}$$

The water depth is constant and the incoming waves are regular first order waves. Therefore the total wave field can be calculated by superposition.

$$\varphi = \varphi_0 + \varphi_s \tag{3}$$

φ_0 is the potential in the undisturbed incoming wave and φ_s is the scattered disturbance due to the presence of the reflectors. Both φ_0 and φ_s satisfies the Laplace equation. The solution to φ_0 is:

$$\varphi_0 = \frac{ag}{\omega}\frac{\cosh k(z+h)}{\cosh kh}\cos(\omega t - kx) \tag{4}$$

In Eq. 4. 2 ω is circular wave frequency, g is acceleration of gravity, t is time, a is wave amplitude, h is water depth and x the position. The wave number k is found from the dispersion relation.

$$\frac{\omega^2}{g} = k\tanh kh \tag{5}$$

The boundary conditions (BC) for φ_s on the water surface, i.e. the kinematic BC (a particle stays on the surface) and the dynamic BC (p=0 in the Bernoulli equation) can be written.

$$\frac{\partial^2\varphi_s}{\partial t^2} + g\frac{\partial\varphi_s}{\partial z} = 0 \qquad \text{, on z=0} \tag{6}$$

At the sea bed no water can flow through the bed, i.e.

$$\frac{\partial\varphi_s}{\partial n} = 0 \qquad \text{, z=-h} \tag{7}$$

In Eq. 7 n is the normal to the sea bed. At the fixed reflector boundary surface S_L the following condition must be fulfilled.

$$\frac{\partial\varphi_s}{\partial n} = -\frac{\partial\varphi_0}{\partial n} \qquad \text{, on } S_L \tag{8}$$

Because the Laplace equation is an epileptic equation the BC's must be given along the whole boundary. At the vertical boundary Sommerfelds radiation condition are used.

$$\frac{\partial\varphi_s}{\partial r} + \frac{1}{c}\frac{\partial\varphi_s}{\partial t} = 0 \qquad ,r\to\infty \tag{9}$$

In Eq. 9 c is the velocity of wave propagation.

As shown by Wehausen and Laitone (1960) it is possible to construct the function $A_E(x,\xi)$ in Eq. 10 in such a way that the boundary conditions at sea bed, water surface and radiation boundary all are fulfilled. This for a pulsating point source.

$$\varphi_{\text{one source}} = f\,A_E(x,\xi)\cos(\delta - \omega t) \tag{10}$$

Where f is source strength, δ is source phase, x is observation point and ξ is position of source. The expression for A_E will not be repeated in this paper.

The reflector surface is discretized into elements with sources at each element and the potential is calculated by superposition of the N sources.

$$\varphi_s = \sum_{j=1}^{N} f_j\,A_E(x,\xi_j)\cos(\delta_j - \omega t) \tag{11}$$

The numerical task is therefore reduced to calculate f_j and δ_j with respect to the surface boundary condition (Eq. 8). This is done at two different times and 2N linear equations for f_j and δ_j are established. How to establish those equations will not be repeated in this paper. When φ_s is known, φ is calculated by Eq. 3.

Wave Power in Linear Regular Waves

From the linearized dynamic free surface condition (Bernoulli equation) the complex amplitude η of the free surface oscillation is derived.

$$\eta(x,y,z) = -\frac{i\omega}{g}\varphi\,, \quad z=0 \tag{12}$$

In Eq. 12 i is imaginary number.

The mean power w due to transport of potential and kinetic energy in a sinusoidal surface gravity wave propagating in deep waters can be calculated per metre width of wave front according to Eq. 13.

$$w = \frac{\rho g^2}{8\pi}Ta^2 \tag{13}$$

In Eq. 13 T is wave period and ρ is mass density of water.

The total mean power W in the cross-section indicated on Fig. 3 is calculated by integration of Eq. 13.

$$W = \int_{-a}^{a} w\,dx \tag{14}$$

Wave Power in Irregular Waves

The irregular waves are transformed by inverse FFT into a sum of N linear waves and the power is calculated as a sum of the power generated by each of these linear waves. The individual waves are given index m and Eq. 14 is now written.

$$W = \sum_{m=1}^{N} \int_{-a}^{a} w_m \, dx \qquad (15)$$

In case of spectral formulated irregular waves, the regular amplitudes are calculated from the spectral density S_η.

$$a_m = 2\int_{f_m}^{f_{m+1}} S_\eta \, df \qquad (16)$$

Numerical tests

The accuracy of the numerical model depends on the chosen meshing. To ensure a decent precision 3 models have been tested with 614, 1494 and 3148 elements. The models were made of quadratic elements with 3, 5 and 7 elements along the wet vertical surface.

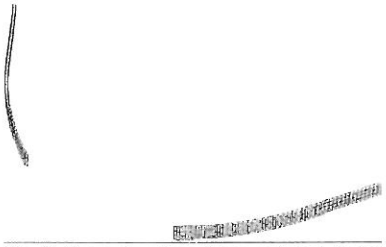

Fig. 7. Example of meshing, original design with 614 elements

The mean power in the cross section is calculated for an incoming wave with amplitude 1meter.

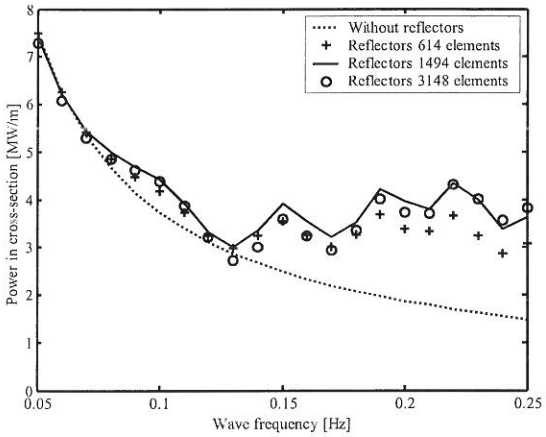

Fig. 8. Mean power at different incoming wave frequencies

Fig. 8 shows that the model with 614 elements seems to underestimate the power at high frequencies. The model with 1494 and 3148 gives almost identical results. The convergence tests shows that the model with 1494 elements produces sufficient accurate results, for which reason it has been used in the subsequent presentation of the results.

LABORATORY EXPERIMENTS

The physical hydraulic model tests were carried out in the 3D wave basin at Aalborg University, Denmark. Approximately in the middle of the wave basin a scale 1:50 reflector-system was connected to thin piles in such a way it was fixed against movements in any direction.

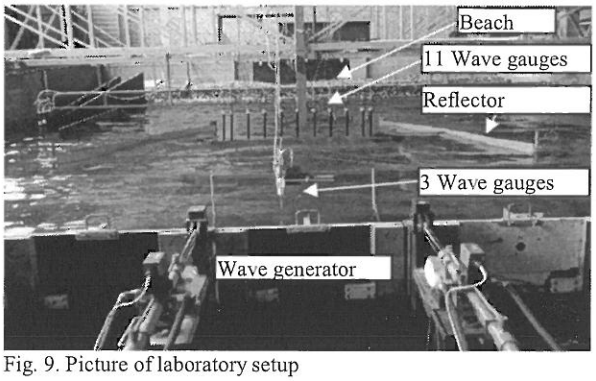

Fig. 9. Picture of laboratory setup

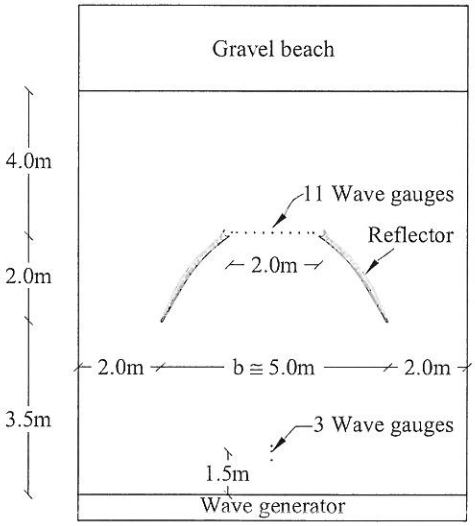

Fig. 10. Plan view of model setup

The relative large reflecting structure causes waves to reflect on the side-walls and wave generator. A visual inspection lead to place 3 wave gauges 1.5 meters in front of the middle of the wave generator. The 3 surface elevation recordings were used to extract the incoming wave from the total wave train. The method proposed by Mansard & Funke (1980) was used to find the incoming wave.

To compare with the numerical model, the results of the laboratory test have been scaled to full scale.

NUMERICAL-EXPERIMENTAL CROSS ANALYSIS

First the original design was tested in regular waves. Fig. 11 shows the surface elevation amplification in the described cross section, this for two different regular waves.

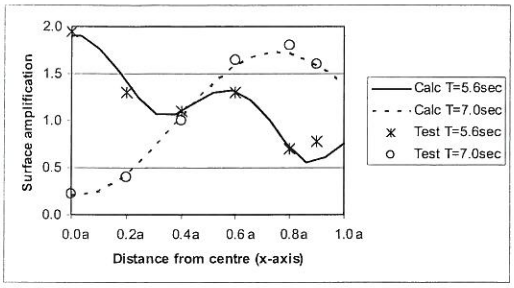

Fig. 11. Behaviour in regular waves

It is seen that the response is very different for the two regular waves. The surface elevation at the centre (0.0a) is very high for the T=5.6sec wave, but for the T=7.0sec wave the surface elevation is very high close to the reflectors (0.8a). A very good agreement between calculated and measured surface amplification is found.

It is clear from Fig. 8 that the efficiency is highest in relatively short waves (high frequencies, low periods). Therefore for the tested irregular waves the performance is best for the low, short waves. It is seen in Table 2 that the reflectors can produce up to approximately 85% more energy in the cross section in case of short waves (Tp = 5.6sec).

Table 2. Performance of original design.

Hs [m]	1	2	3	4	5
Tp [sec]	5.6	7.0	8.4	9.8	11.2
Calc. efficiency [%]	185	145	124	120	115
Test efficiency [%]	186	163	125	117	106

Generally a very good agreement between calculated and measured efficiencies is found. The differences in calculated and test efficiencies are mainly due to the definition of the incoming wave in the laboratory. Longer waves in the laboratory cause more reflection. For the short waves the reliability of the incoming waves are therefore better.

In Table 1 it is seen that in the Danish part of the North Sea the short waves are most likely. But it is also seen that the short waves only contain a small amount of energy. For the original design the yearly averaged efficiency at a typical location in the North Sea is 130%.

The yearly averaged efficiencies are calculated for the designs with rotated reflectors and the results are compared in Table 3, Fig. 12 and Fig. 13. Those graphs are valid for the reflector length of 125m (indicated on Fig. 1 and Fig. 5). It is clear that the original design does not give the optimal efficiency in the cross section.

Table 3. Performance of designs with rotated reflectors.

Rotation of reflectors	+10°	+5°	0°	-5°
b/a	2.27	2.41	2.60	2.80
L/(b-a)	1.75	1.50	1.25	1.04
Calc. efficiency [%]	-	140	130	118
Test efficiency [%]	130	136	131	-

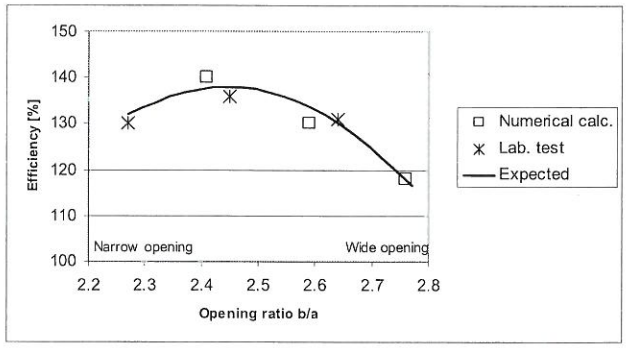

Fig. 12. Efficiencies for rotated reflectors, length of reflectors = 125m

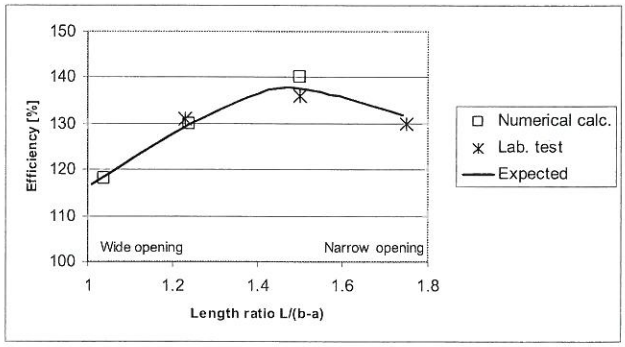

Fig. 13. Efficiencies for rotated reflectors, length of reflectors = 125m

The top point of the graphs on Fig. 12 and Fig. 13 corresponds to a rotation of approximately +5° compared to the original design.

The influence of the length of the reflectors is shown in Fig. 14. The extension is related to the original length of 125m.

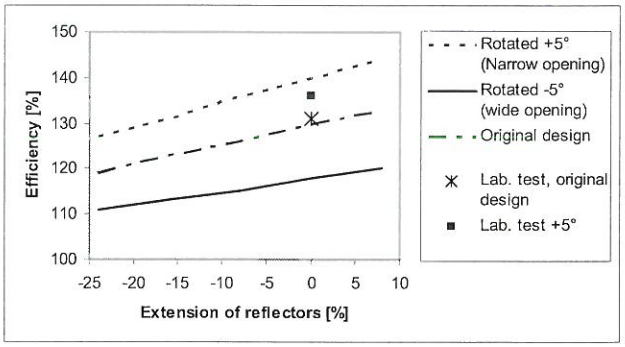

Fig. 14. Efficiencies for extended reflectors

It is clear from Fig. 14, that the longer reflectors, the greater is the efficiency.

All the results have been plotted in Fig. 15 and the areas are split up in parts with efficiencies of 100-110%, 110-120%, 120-130%, 130-140% and 140%→. For a given WEC-layout with specified length of cross-section, Fig. 15 can be used to evaluate approximate benefit for different reflector layouts.

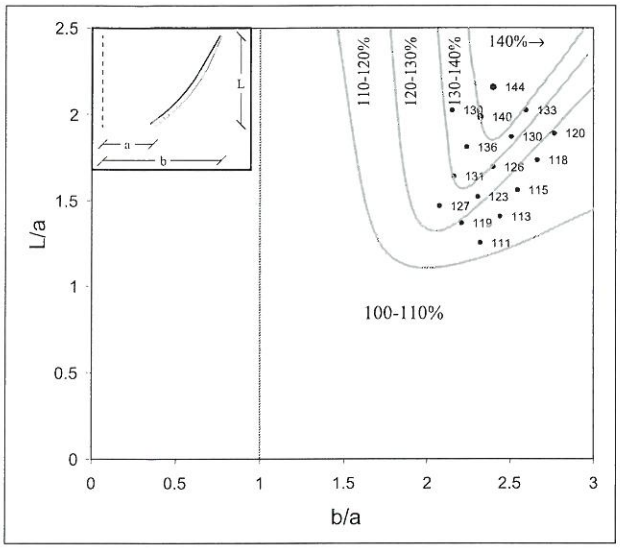

Fig. 15. Correlation between efficiency and reflector layout

CONCLUSIONS

15 different geometrical setups of different layouts of floating reflectors have been investigated in both regular waves and 5 irregular wave situations. The following main conclusions may be drawn:

- Floating wave reflectors used for wave energy focussing can increase the total amount of energy in a cross section to approximately 130-140%.
- A very good agreement between laboratory experiments and numerical results is found. The numerical BEM has therefore proved to be an efficient, fast and simple method to optimize reflector designs.
- The BEM has been used to optimize the wave reflectors for the wave energy converter *Wave Dragon.*

REFERENCES

Faltinsen, OM (1990). "Sea Loads on Ships and Offshore Structures," Cambridge University Press.

Kofoed, JP, Frigaard, P, Soerensen, HC, and Friis-Madsen, E (2000). "Development of the Wave Energy Converter – Wave Dragon," *Int J Offshore and Polar Eng*, ISOPE, vol 1, No 10, pp 405-412.

Mansard, E and Funke, E (1980). "The Measurement of Incident and Reflected Spectra Using a Lease Squares Method," *Proceedings, 17th International Conference on Coastal Engineering*, Vol. 1, pp 154-172, Sydney, Australia.

Soerensen, HC, Hansen, R, Friis-Madsen, E, Panhauser, W, Mackie, G, Hansen, HH, Frigaard, P, Hald, T, Knapp, W, Keller, J, Holmén, E, Homes, B, Thomas, G, Rasmussen, P, and Krogsgaard, J (2000). "The Wave Dragon – Now Ready for Test in Real Sea," *Fourth European Wave Energy Conference*, No G1.

Wehausen, JV and Laitone, EV (1960). "Surface Waves," *Handbuch der Physik*, ed. S. Flügge, Springer Verlag, Berlin, Vol IX, pp 446-778.